Available online at www.sciencedirect.com
SCIENCE DIRECT
Carbohydrate Polymers 61 (2005) 455–463
Carbohydrate Polymers
www.elsevier.com/locate/carbpol

# Thermoplastic starch–clay nanocomposites and their characteristics

Biqiong Chen, Julian R.G. Evans*

*Department of Materials, Queen Mary, University of London, Mile End Road, London E1 4NS, UK*

Received 26 January 2005; revised 9 May 2005; accepted 16 June 2005
Available online 9 August 2005

**Abstract**

In the quest for improved performance from polymers that offer biodegradation and therefore environmental acceptability, one approach is the addition of natural clays to produce nanocomposites. This study examines nanocomposites of glycerol-plasticized starch, with untreated montmorillonite and hectorite. Treated hectorite and kaolinite were added to produce conventional composites within the same clay volume fraction range for comparison. X-ray diffraction and transmission electron microscopy are used to confirm the type of composite. The ultrasonic pulse-echo technique was used to measure Young's and shear modulus. The nanocomposites presented greater increases in modulus for a given volume fraction of clay thus contributing to this new class of biodegradable and environmentally acceptable materials, although the results indicate that a plasticizer other than glycerol is preferable.


*Keywords:* Starch; Nanocomposite; Clay; Morphology; Elastic modulus

## 1. Introduction

Biodegradable polymers such as starch (Arvanitoyannis, Biliaderis, Ogawa, & Kawasaki, 1998; Arvanitoyannis, Kolokuris, Nakayama, & Aiba, 1997; Psomiadou, Arvanitoyannis, Biliaderis, Ogawa, & Kawasaki, 1997), poly(lactide) (Ray et al., 2002, 2003; Krikorian & Pochan, 2003) and poly(ε-caprolactone) (Gaudel-Siri et al., 2003; Jimenez, Ogata, Kawai, & Ogihara, 1997; Kubies, Pantoustier, Dubois, Rulmont, & Jerome, 2002), have attracted considerable attention in the packaging industry. Starch is a promising raw material because of its annual availability from many plants, its rather excessive production with regard to current needs and its low cost (Gonera & Cornillon, 2002; Smits, Ruhnau, Vliegenthart, & van Soest, 1998). It is known to be completely degradable in soil and water and can promote the biodegradability of a non-biodegradable plastic when blended. Starch is commonly pretreated with a plasticizer to make it thermoplastic thus enabling melt-processing.

However, thermoplastic starch (TPS) alone often cannot meet all the requirements of a packaging material and an environmentally acceptable filler is called for to improve the properties of TPS in such applications. Clay is a potential filler; itself a naturally abundant mineral that is toxin-free and can be used as one of the components for food, medical, cosmetic and healthcare recipients (Bakraji & Karajou, 2003; Jinadasa & Dissanayake, 1992; Pang, Fan, Liu, Chen, & Li, 2003; Qian et al., 2002).

TPS reinforced by clay has recently been investigated (De Carvalho, Curvelo, & Agnelli, 2001; McGlashan & Halley, 2003; Park et al., 2002; Park, Lee, Park, Cho, & Ha, 2003; Wilhelm, Sierakowski, Souza, & Wypych, 2003). To the authors' knowledge, there are just four publications describing this new class of materials, i.e. TPS–clay nanocomposites. Starch is hydrophilic and forms nanocomposites with natural smectite clays (Park et al., 2002, 2003; Wilhelm et al., 2003) and conventional composites with kaolinite (De Carvalho et al., 2001). It has been shown that the tensile strength of TPS was increased from 2.6 to 3.3 MPa with the presence of 5 wt% sodium montmorillonite, while the elongation at break was increased from 47 to 57% (Park et al., 2003). Also the relative water vapour diffusion coefficient of TPS was decreased to 65% and the temperature at which the composite lost 50% mass was increased from 305 to 336 °C (Park et al., 2003).

* Corresponding author. Tel.: +44 20 7882 5501; fax: +44 20 8981 9804.
*E-mail address:* j.r.g.evans@qmul.ac.uk (J.R.G. Evans).

0144-8617/$ - see front matter © 2005 Elsevier Ltd. All rights reserved.
doi:10.1016/j.carbpol.2005.06.020

The present work sets out to prepare and characterize starch–clay nanocomposites with clays that can act as hosts at a range of volume fractions and to compare the results with similar clays that do not host starch.

## 2. Experimental details

### 2.1. Materials

Four clays were used to prepare composites of different types with thermoplastic starch. Natural sodium montmorillonite (type: BH natural) with a density of 2600 kg $m^{-3}$ and outer specific surface area (measured by B.E.T. nitrogen adsorption) of 38 $m^2$ $g^{-1}$ was obtained from Blackhill Bentonite LLC (Wyoming, USA). Natural hectorite (type EA-163) with a density of 2600 kg $m^{-3}$ and outer specific surface area of 50 $m^2$ $g^{-1}$ and hectorite modified with 2 methyl, 2 hydrogenated tallow quaternary ammonium chloride (type: Bentone 109) with a density of 1700 kg $m^{-3}$ were obtained from Elementis Specialties (Hightstown, USA). Both montmorillonite and hectorite are among the most common smectite clay minerals and they are members of dioctahedral and trioctahedral groups, with ideal chemical formulae of $Al_4Si_8O_{20}(OH)_4 \cdot nH_2O$ and $Mg_6Si_8O_{20}(OH)_4 \cdot nH_2O$, respectively (Grim, 1968). Kaolinite (type: Plus white) with ideal composition of $Al_4Si_2O_{10}(OH)_8$ and a density of 2580 kg $m^{-3}$ and outer specific surface area of 24 $m^2$ $g^{-1}$ was obtained from Charles B. Crystal Co. (New York, USA). Potato starch and glycerol were from VWR International (Leicestershire, UK). The moisture content of starch was 1.7 wt% as determined by drying to constant mass. All materials were used without further modification.

### 2.2. Preparation of composites

Thermoplastic starch was prepared by melt-processing of starch and glycerol at a ratio of 10:3 by mass according to previous studies on the optimized ratio (De Carvalho et al., 2001). The pristine starch and glycerol were premixed allowing the plasticizer to swell the starch powder. The mixture was then transferred to a twin roll mill (Carter International, Rochdale, UK) and mixed at 120 °C. The rolls were heated with an oil heater (model: SHK 300 09 Tricool Engineering Ltd, Hants, UK). To ensure lateral mixing, the mixture was stripped from the rolls and re-fed at least five times, which took approximately 15 min. To prepare the TPS–clay composites, pre-weighed amounts of clay were gradually added to the polymer melt on the twin roll mill. The mixing procedure was as above. The specimens for ultrasonic testing and X-ray diffraction (XRD) were pressed in moulds at 120 °C under a pressure of 27 MPa for 60 s using a hydraulic press.

Glycerol–clay and starch–clay mixtures were prepared in the presence of distilled-water. Clay was first mixed with distilled water to form a 0.05 g $ml^{-1}$ suspension which was agitated for 5 h on a roller table. A known amount of glycerol or starch (organic:inorganic = 0.6 by mass) was added to pre-prepared clay dispersion and mixed for a further 5 h before casting into a petri dish. The resulting products were dried at 60 °C in an air-circulating oven.

### 2.3. Characterization

The clay contents in the melt-processed composites were determined by loss on ignition. The composites were heated in air to 600 °C at 10 °C $min^{-1}$ in a muffle furnace (Lenton Thermal Design Ltd, Sheffield, UK) and after a dwell of 10 min furnace cooled to 20 °C. The residue was weighed after storing in air at 20 °C for 8 h. As-received clays were also fired and weighed to adjust for water loss.

A Siemens D5000 X-ray diffractomer (40 kV, 40 mA) with Cu K$\alpha$ radiation ($\lambda = 0.154$ nm) was used for XRD measurements. The aperture slits were set at 0.1° and the scanning step was 0.02° with a scan time of 2.5 s per step. Measurements were conducted on moulded plates.

Scanning electronic microscopy (SEM) on fracture surfaces was performed on a JSM6300 JEOL WINSEM with an operating voltage at 10 kV. All the specimens were sputter-coated with gold. Transmission electron microscopy (TEM) was conducted on a JEOL JEM 2010 electron microscope, operating at 200 kV, and with Kodak SO-163 film. TEM specimens of starch–clay composites were prepared by dispersing the composite powders in acetone by ultrasonicating. The grids were 300-mesh carbon-coated.

Solid state nuclear magnetic resonance (NMR) was conducted at ambient temperature on a Bruker AV600 spectrometer operating at 600 MHz. The sample was run in a 4 mm (internal diameter 3.7 mm) diameter MAS rotor which is approximately 10 mm long. Typically about 100 mg was used to fill the rotor; about 10 mg sample was added at a time and pressed into the rotor with a metallic tool. The MAS spinning rate was 10,000 Hz, the 90° pulse width was 3.7 μs and the ramped CP pulse was 1 ms. TPPM15 decoupling of $^1H$ was used and the $^1D$ spectrum of $^{13}C$ was run with spinning sideband suppression according to Dixon, Schaefer, Sefcik, Stejskal, and McKay (1982).

Elastic constants of polymer–clay nanocomposites were calculated from ultrasonic measurements with the pulse-echo mode using a 500PR ultrasonic pulser/receiver (Panametrics NDT Ltd, Rotherham, UK) and a TDS200 digital real-time oscilloscope (Tektronix, Beaverton, USA). Measurements were calibrated with a surface ground steel step-wedge and conducted on the cuboids (50 mm × 50 mm × 5 mm) with parallel surfaces

prepared by a hydraulic press. Shear modulus $G$, Poisson's ratio $\upsilon$ and Young's modulus $E$ were calculated using Eqs. (1)–(3) (Krautkrämer & Krautkrämer, 1990):

$$G = \rho C_t^2 \quad (1)$$

$$\upsilon = \frac{(1/2)(C_l/C_t)^2 - 1}{(C_l/C_t)^2 - 1} \quad (2)$$

$$E = 2(\upsilon + 1)G \quad (3)$$

where $\rho$ is the density of the test specimen, and $C_l$ and $C_t$ are the transmission velocities under longitudinal and transverse sonic waves, respectively. They are equal to the path length (twice the sample height) divided by the time between transmission and detection of the pulse which can be measured from the neighbouring peak distance.

## 3. Results and discussion

Conventional composites and nanocomposites of TPS–clay were prepared with four types of clay by melt-processing. The nominal mass fractions of the clays and composites were determined by loss on ignition and the results are shown in Table 1. During melt-processing, it became clear that 10 vol.% untreated clay was approximately the maximum loading that this TPS could sustain.

Table 1
Compositions of TPS–clay composites deduced form loss on ignition

| Sample designation | Average mass fraction of residue[a] | Mass fraction of clay | Nominal volume fraction of clay[b] |
|---|---|---|---|
| TPS | 0.004 | 0 | 0 |
| Montmorillonite | 0.94 | – | – |
| M3 | 0.05 | 0.06 | 0.029 |
| M7 | 0.13 | 0.13 | 0.071 |
| M10 | 0.17 | 0.18 | 0.098 |
| M12 | 0.20 | 0.22 | 0.120 |
| Hectorite | 0.89 | – | – |
| H2 | 0.04 | 0.05 | 0.024 |
| H7 | 0.12 | 0.13 | 0.070 |
| H10 | 0.17 | 0.19 | 0.107 |
| H11 | 0.18 | 0.20 | 0.108 |
| Treated hectorite | 0.60 | – | – |
| TH2 | 0.03 | 0.05 | 0.018 |
| TH3 | 0.06 | 0.09 | 0.031 |
| TH4 | 0.08 | 0.13 | 0.043 |
| TH7 | 0.11 | 0.19 | 0.065 |
| Kaolinite | 0.87 | – | – |
| K3 | 0.04 | 0.05 | 0.025 |
| K6 | 0.09 | 0.11 | 0.055 |
| K9 | 0.15 | 0.17 | 0.094 |
| K10 | 0.16 | 0.18 | 0.098 |

[a] Refers to the mass fraction of clay platelets for the nanocomposites.
[b] The nominal volume fractions of treated hectorite composites are corrected to give the loadings of untreated hectorite.

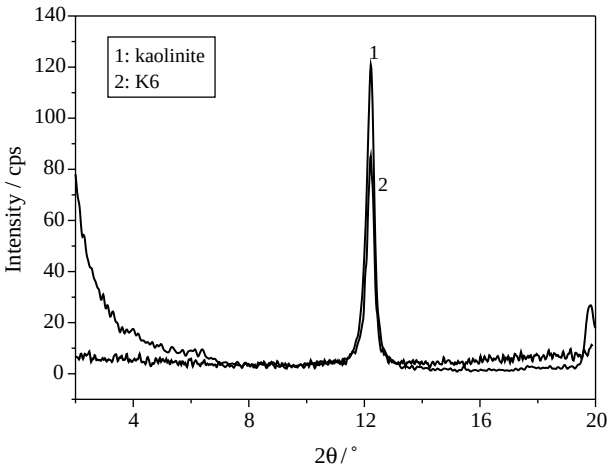


Fig. 1. XRD traces of kaolinite and thermoplastic starch–kaolinite conventional composite containing 9 wt% clay platelets (K6).

This loading is somewhat lower than that sustained by poly(ethylene glycol) (Chen & Evans, 2005) and poly(ε-caprolatone) (Chen and Evans, in press), mainly because of the different wetting and viscosity characteristics of TPS.

Unlike natural montmorillonite and hectorite, kaolinite is a non-swelling clay and should produce conventional composites with the starch. That kaolinite formed conventional composites with TPS was confirmed by XRD. Fig. 1 shows that the (001) peak of the kaolinite does not shift after mixing with TPS; $d_{001}$ remained at 0.72 nm indicating no intercalation.

Fig. 2 shows XRD traces for TPS–montmorillonite nanocomposites and a glycerol–montmorillonite mixture. The (001) peak of the clay was displaced from 7.16° of $2\theta$ to 4.9° for each composition of TPS–clay nanocomposite, correspondingly to an increase of $d_{001}$ from 1.23 to 1.8 nm. The broad 001 peak suggests a wide range of interlayer

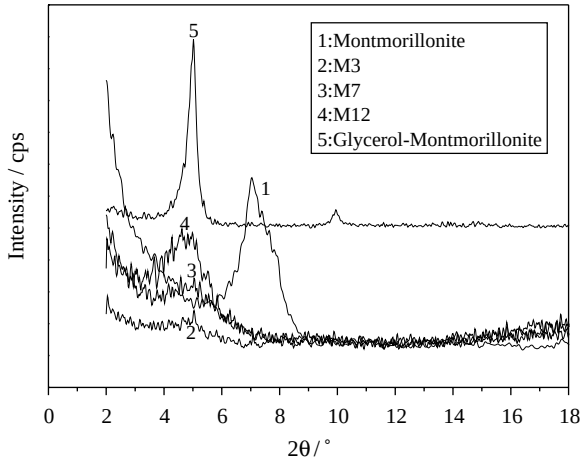


Fig. 2. XRD traces of thermoplastic starch–montmorillonite nanocomposites containing 5, 13 and 20 wt% clay platelets (M3, M7 and M12) and of the glycerol–montmorillonite mixture.

spacings. This is further supported by TEM images showing co-existence of intercalation and exfoliation and is discussed below. In comparison, the (001) peak of montmorillonite was displaced to 5° of $2\theta$ after mixing with glycerol (curve 5), suggesting the uptake of glycerol into the clay galleries. The glycerol produced a sharper (001) peak indicative of a more ordered structure for the clay containing glycerol.

Many polymers when taken up by montmorillonite produce an expanded structure with $d \approx 1.8$ nm (Aranda & Ruiz-Hitzky, 1992; Shen, Simon, & Cheng, 2002; Triantafillidis, LeBaron, & Pinnavaia, 2002). The fact that glycerol also produces this $d$-spacing, makes it difficult to assess, on the basis of Fig. 2 whether starch and glycerol entered into the galleries or just glycerol. The significant differences in the peak width between glycerol treated starch and glycerol composites and the slightly larger $d_{001}$ for glycerol–starch suggest the former. This is supported by the fact that the untreated clay exfoliates in water-plasticized starch as shown in the literature (Wilhelm et al., 2003) and the discussion below.

Fig. 3 shows XRD traces for starch–untreated hectorite and glycerol–untreated hectorite mixtures. As with montmorillonite, the (001) peak of the hectorite was displaced from 7.16° of $2\theta$ to 4.9° for both the TPS–clay composites (H3, H7) implying intercalation. The as-received hectorite has a slightly wider (001) peak compared with montmorillonite but both the TPS–hectorite nanocomposites had sharper (001) peaks (width at half height of peak: 1.1° of $2\theta$ versus 1.6°) than the montmorillonite nanocomposites, indicating that these nanocomposites had more layer coherence. The intercalation of glycerol into the clay galleries increased $d_{001}$ from 1.23 to 1.8 nm as it did with montmorillonite. However, the (001) peak was not detected in water-plasticized starch–hectorite mixtures (curve 5) and this may be indicative of exfoliation; certainly it was not due to low clay content because the mixture contained 62.5 wt% clay. Wilhelm et al. (2003) attributed the loss of (001) peak to full exfoliation under similar conditions. The addition of glycerol as plasticizer may have inhibited complete exfoliation of clay platelets but a non-volatile plasticizer is essential for processing useful starch-based materials; without it the mixture of starch and clay powders cannot cohere after the evaporation of water.

Treatment of clay with glycerol alone increases the interlayer spacing by 0.6 nm. During plasticizing, glycerol, like water, forms hydrogen bonds with native starch (Trommsdorff & Tomka, 1995) and as this association took place during mixing before clay addition it is probable that the glycerol-plasticized system intercalated. Under similar circumstances, the water-plasticized systems exfoliated. In fact, starch also encouraged some clay platelets to exfoliate, creating a glycerol-plasticized composite with partial intercalation and partial exfoliation as implied by the wide (001) peaks in Figs. 2 and 3.

XRD traces of starch with treated hectorite mixtures are shown in Fig. 4. As the diffractometer was used at its low angle limit, it is difficult to determine the exact positions for the (001) peak in some cases. However, it can be seen that the $2\theta$ position of the (001) peak for the treated hectorite remained almost the same after mixing with TPS. The mixture of glycerol and treated hectorite gave a similar $d_{001}$ to that of the treated clay. In this circumstance, whether the TPS causes some clay platelets to exfoliate, or just provides conventional composites with the clay is still unknown. The simplest reading of Fig. 4 is that conventional composites are formed. Other techniques are required to confirm the class of these composites as discussed below.

Fig. 5 shows the TEM image of the TPS–untreated hectorite nanocomposite containing 4 wt% clay platelets. The silicate layers exist mostly as either single platelets (exfoliation) or as stacks of several platelets (intercalation). This is coincident with the relatively broad and small (001)

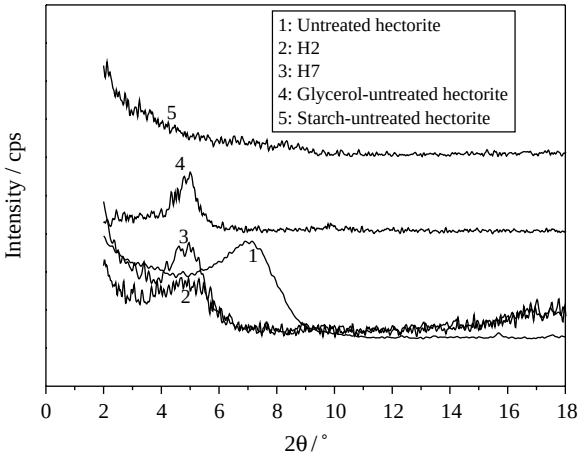


Fig. 3. XRD traces of thermoplastic starch–untreated starch–untreated hectorite nanocomposites containing 4 and 12 wt.% clay platelets (H2 and H7); glycerol–untreated hectorite and water-plasticized starch–untreated hectorite mixtures.

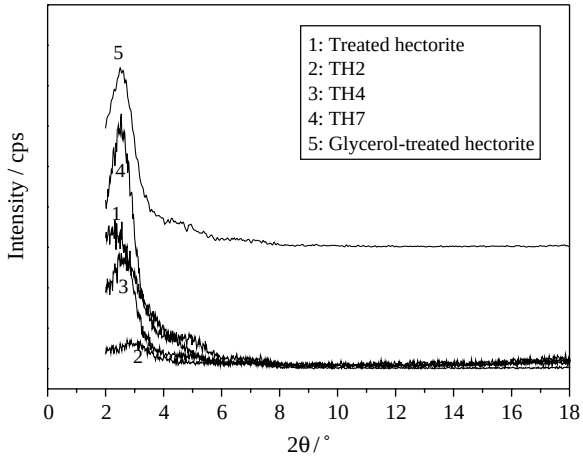


Fig. 4. XRD traces of thermoplastic starch–treated hectorite composites containing 3, 8 and 11 wt% clay platelets (TH2, TH4 and TH7), and glycerol–treated hectorite mixture.

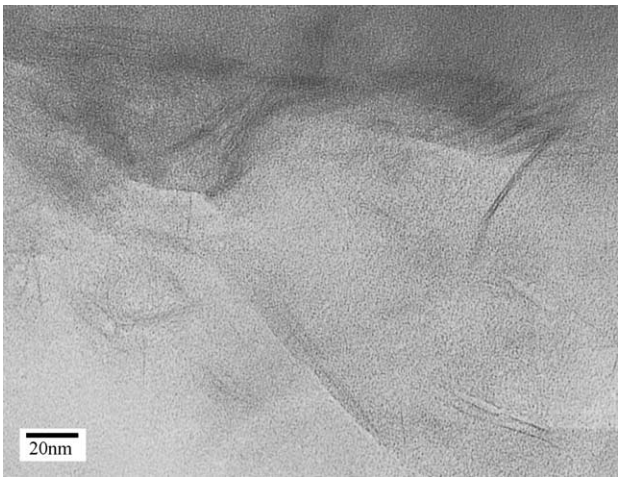


Fig. 5. TEM micrograph of thermoplastic starch–untreated hectorite nanocomposite containing 4 wt% clay platelets (H2).

peak in Fig. 3. The length of the single silicate platelet is between 10 and 50 nm, shorter than that of montmorillonite (Chen & Evans, 2005) and consistent with the larger outer specific surface area measured by B.E.T. nitrogen adsorption (50 versus 38 $m^2\ g^{-1}$).

Fig. 6 shows the TEM micrographs of the treated hectorite and the TPS–treated hectorite composite. The treated hectorite (the hectorite intercalated with quaternary ammonium chloride) itself includes both exfoliated and intercalated structures, visible as some single clay platelets and some clay tactoids from the TEM image (Fig. 6a). The TPS–treated hectorite composite also has these two structures (Fig. 6b), however, it is not possible to compare the extents of intercalation and exfoliation with the unfilled treated hectorite under TEM because the numbers of clay platelet per stack are very similar.

In the images for the TPS–treated hectorite composite, large dark regions were often seen and they also appear in Fig. 6b. These regions are attributed to thick large particles, which suggest the formation of clay agglomerates in the composites. This indicates that the hydrophilic thermoplastic starch is not able to interact with the organophilic ammonium-treated clay strongly and the clay particles cannot disperse well in the continuous phase. Thus although some clay platelets were exfoliated, the composite is generally a conventional one rather than a nanocomposite and this is further supported by the mechanical properties which show that the TPS–treated clay composites had lower elastic moduli than those nanocomposites with untreated hectorite and at a similar clay platelet loading.

The TEM sample preparation method used here is not ideal; the ultramicrotome available uses a water bath and therefore cannot be employed for starch. Carrado, Xu, Seifert, Csencsits, and Bloomquist (2000) prepared polyacrylonitrile-clay samples by ultrasonicating the composites in methanol. Acetone, with a lower solubility parameter (19.7 $MPa^{1/2}$) than methanol (29.7 $MPa^{1/2}$) (Barton, 1983)

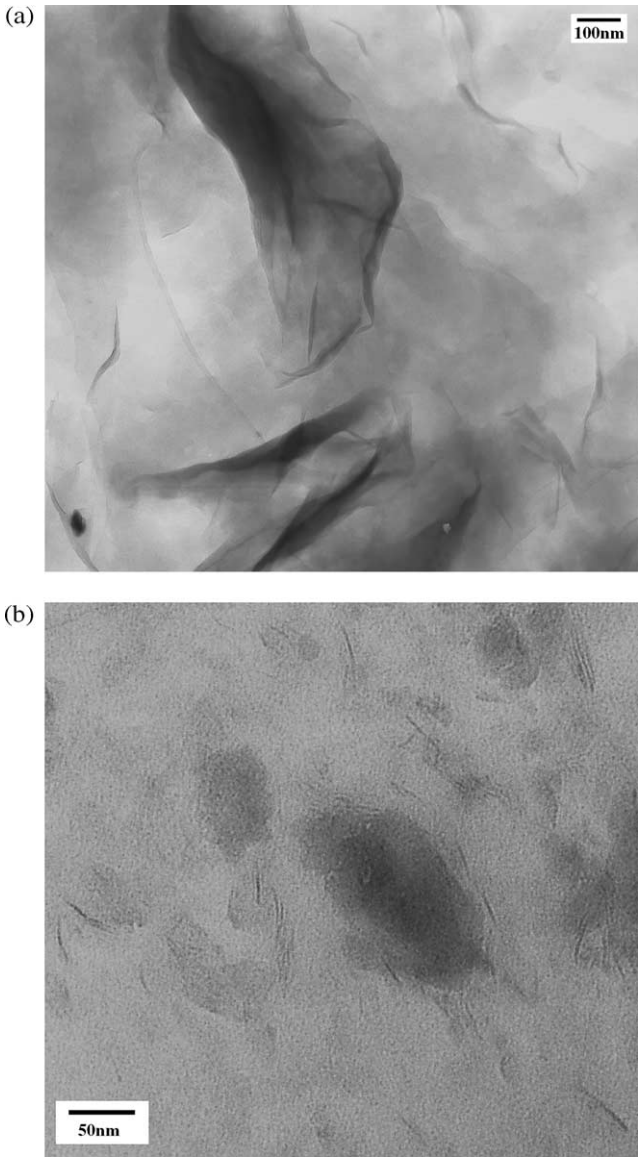


Fig. 6. TEM micrographs of (a) treated hectorite, and (b) TPS–treated hectorite composites containing 3 wt% clay platelets (TH2).

was selected here but could still, when assisted by ultrasound, affect the microstructure of clay perhaps by dissolving some glycerol molecules and hence collapsing the layers. The TEM images therefore provide only a qualitative assessment of clay dispersion but are consistent with the XRD results and mechanical property measurements discussed below.

Fig. 7a shows the NMR spectra of the starch and starch–montmorillonite nanocomposites. The chemical shifts at 60.8, 71.9, 80.9 and 101.1 ppm represent the carbons of type VI, II (and III, V), IV and I as numbered in Scheme 1 (Smits et al., 1998; Tavares, Bathista, Silva, Filho, & Nogueira, 2003).

The spectrum for the native starch remained nearly unchanged after the addition of montmorillonite, implying that the presence of montmorillonite did not affect the structure of starch although the inorganic

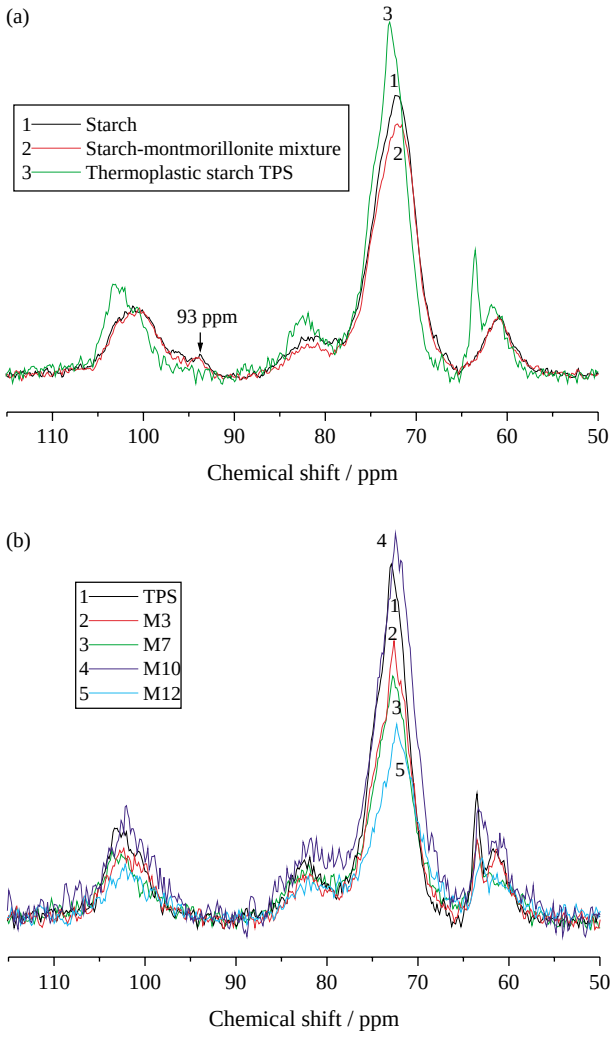


Fig. 7. NMR spectra of starch, starch–montmorillonite, TPS and TPS–montmorillonite nanocomposites containing 5, 13, 17 and 20 wt% clay platelets (M3, M7, M10 and M12).

montmorillonite itself experiences the exfoliation of platelets from the bulk particles. The new peak at 63.5 ppm in the spectrum for the plasticized starch (Curve 3) may be attributed to the carbon in glycerol. Also the peak for C1 anomeric carbon at 102 ppm is wide and does not include the small peak at 93 ppm as present in native starch, suggesting the starch has been de-structured during gelatinisation (Smits et al., 1998).

At low clay contents ($\leq$13 wt%), the addition of montmorillonite to TPS did not alter the peak positions; only the intensity was changed (Fig. 7b). At higher clay loadings, the upfield peak shift of 0.6 ppm due to interaction between clay and polymer is easily detected.

Elastic moduli of thermoplastic starch–clay composites are plotted against nominal clay volume fractions and they are shown in Fig. 8. The nominal volume fractions of treated clay were corrected to the content of untreated hectorite as shown in Table 1. The measurement error in modulus was within 5% as deduced from the steel calibration gauges.

In all composites, the presence of clay increased both Young's and shear modulus, and the montmorillonite and unmodified hectorite provided significantly more increase than kaolinite which formed conventional composites with TPS. That the treated-hectorite composites had similar elastic moduli to those prepared from kaolinite which gives conventional composites, supports the previous observation that they also formed conventional composites. Hectorite particles have a lower aspect ratio and larger surface area than montomorillonite, the former factor tending to give a smaller modulus increase and the latter giving a greater increase. Thus it is difficult to predict which clay will give

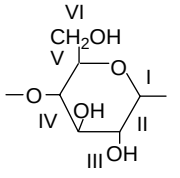


Scheme 1. Identification of carbons in α-D-glucose (the repeat unit of the polymers that made up of starch).

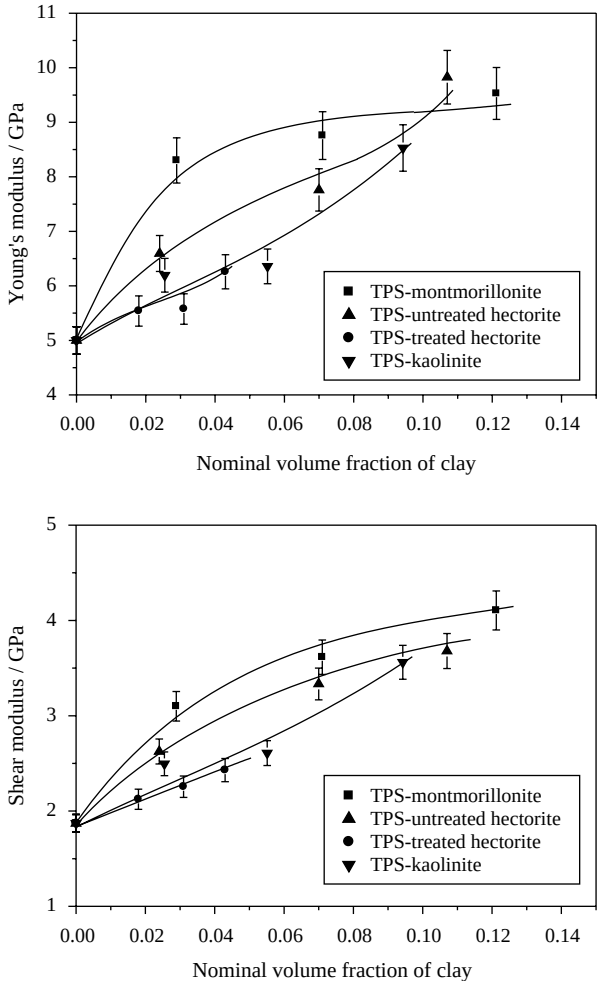


Fig. 8. Young's modulus and shear modulus of TPS–clay composites (Error bars represent 5% error inherent in the measurement).

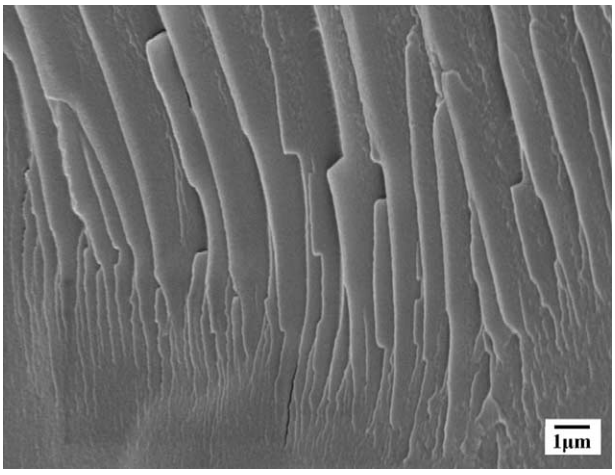


Fig. 9. SEM image on fractured surfaces of TPS–hectorite nanocomposite disc fractured after storage for 30 days.

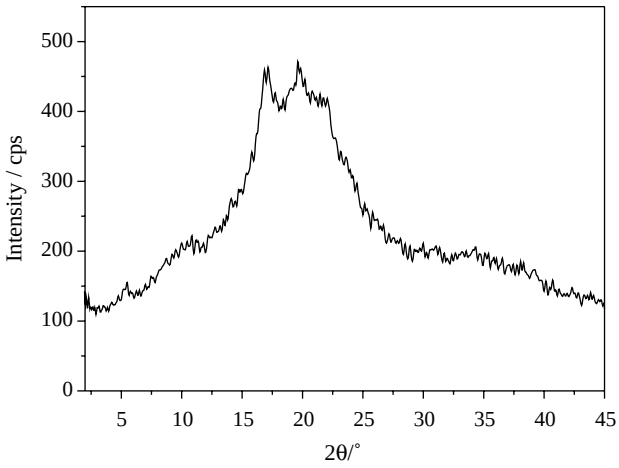


Fig. 10. XRD trace of the thermoplastic starch stored for 80 days showing recrystallisation.

better property enhancement without applying detailed models.

At low clay fractions, montmorillonite provided a higher Young's modulus than the hectorite composite but at higher clay fractions, reinforcement deteriorated. Nevertheless, it is clear that a nanocomposite provides a higher modulus than a conventional composite with the same clay content. SEM image of the fracture surface of a TPS–clay composite is shown in Fig. 9. Like unfilled TPS, all the TPS–clay composites showed crazing on the fracture surfaces. Although this work points the way to potential environmentally acceptable materials, the composition requires further refinement notably in terms of the selection of plasticizer. Except for TPS–treated hectorite composites, both the composites and the unfilled TPS samples exhibited cracking after storage for 80 days, which can be attributed to progressive recrystallisation. It is noteworthy that consistent ultrasonic tests were conducted twice; after 7 days and again after 13 days past-preparation and that no cracks were visible at these times. Ma and Yu (2004) found that glycerol plasticized starch presented increased crystallinity after storing at RH = 0 and 50% for 25 days. Smits et al. (1998) found that such retrogradation also occurred to water-plasticized starch and they attributed the embrittlement problem to recrystallisation (retrogradation). The alkylammonium salt as the modifier for hectorite may have inhibited the occurrence of recrystallisation. However, Calvert (1997) attributed the cracking problem to the evaporation of plasticizer. Ma and Yu (2004) recently reported that starch plasticized with urea did not present the retrogradation problem. They found that the retrogradation of thermoplastic starch was dependent on the capability for hydrogen bond formation between plasticizer and starch. The stronger the hydrogen bond, the more difficult it is for starch to recrystallise during storage. The $NH_2$-bond in an alkylammonium salt is thought to form a strong hydrogen bond with starch.

The XRD trace of the thermoplastic starch after 80 day's storage (Fig. 10) shows two small peaks between 15 and 25° of $2\theta$, supporting the hypothesis of the occurrence of recrystallisation. These peaks are similar to those reported by Ma and Yu (2004) who showed the stored TPS had a greater crystallinity than the freshly-prepared; after 25 day's storage, two small peaks appeared at 16.96 and 19.68° on the top of the original wide peak.

Water absorption of TPS and the TPS–clay nanocomposite containing 6 wt% montmorillonite was studied according to ASTM D570. After immersing in distilled water for 2 h, the unfilled TPS became very soft and loose due to partial dissolution and swelling causing some of the material to disperse in water. However, the nanocomposite remained generally intact after the same immersion conditions. These results imply that the presence of clay enhances the water resistance of TPS although exact water absorption data were not obtained.

Since the problem of embrittlement during storage causes these TPS–clay composites to be unsuitable for long-term use, it seems important to replace this commonly-used plasticizer for starch, namely glycerol, with other suitable hydrogen bonding plasticizers. On the grounds that ammonium-treated hectorite inhibits the embrittlement problem of TPS, one might speculate that a plasticizer containing $NH_4^+$ ions or $NH_2^-$ would not experience cracking problems. The added value in using this kind of plasticizer is that the plasticized starch might be compatible with ammonium-treated clays and thus provide more possibilities for forming exfoliated nanocomposites. In this way, thermoplastic starch–clay nanocomposites with high elastic moduli could be produced. The ammonium-treated clay also increased the optical clarity of the unfilled TPS, thus such thermoplastic starch–clay nanocomposites are also expected to have good optical clarity.

## 4. Conclusions

TPS–clay composites with various types of clay and clay loadings were easily prepared by melt-processing on the twin roll mill. The natural smectite clays, montmorillonite and hectorite, readily formed nanocomposites with TPS as characterized by XRD, which showed wide (001) peaks and enlarged $d_{001}$ of 1.8 nm for the intercalated clay. The unchanged $d_{001}$ of kaolinite indicates that kaolinite formed conventional composites with TPS. TEM showed the untreated hectorite nanocomposites are partially exfoliated while the TPS–treated hectorite composites are conventional. The interaction between glycerol-plasticized starch and montmorillonite is detected by NMR at the higher clay loadings. In all cases, clay increased the elastic modulus of TPS. The moduli of treated-hectorite and kaolinite composites were very similar at similar clay loadings and were lower than the nanocomposites, indicating that these are conventional composites in agreement with TEM observations. For nanocomposites, montmorillonite generally provided a slightly greater improvement in the modulus than untreated hectorite. TPS with and without natural clay underwent cracking during prolonged storage attributable to recrystallisation of TPS as evidenced by XRD. TPS–treated hectorite did not present this cracking problem but it does indicate that an alternative plasticier should be found.

## Acknowledgements

This work is supported by the Engineering and Physical Science Research Council in the UK under grant no. GR/R30907. Lei Feng is thanked for participation in sample preparation, and some SEM imaging and ultrasonic testing. We are grateful for helpful discussions with Peter Coveney (University College London) and Andy Whiting (Durham University) and to Harold Toms (Queen Mary, University of London) for operating the NMR instrument.

## References

Aranda, P., & Ruiz-Hitzky, E. (1992). Poly(ethylene oxide)-silicate intercalation materials. *Chemistry of Materials*, *4*, 1395–1403.

Arvanitoyannis, I., Biliaderis, C. G., Ogawa, H., & Kawasaki, N. (1998). Biodegradable films made from low-density polyethylene, rice starch and potato starch for food packaging applications: Part 1. *Carbohydrate Polymers*, *36*, 89–104.

Arvanitoyannis, I., Kolokuris, I., Nakayama, A., & Aiba, S.-I. (1997). Preparation and study of novel biodegradable blends based on gelatinised starch and 1,4-*trans*-polyisoprene (gutta percha) for food packaging or biomedical applications. *Carbohydrate Polymers*, *34*, 291–302.

Bakraji, E. H., & Karajou, J. (2003). Determination of trace elements in Syrian bentonite clay using X-ray fluorescence technique and discussion on the health implication on pregnant women. *Journal of Trace and Microprobe Techniques*, *21*(2), 397–405.

Barton, A. F. M. (1983). *Handbook of solubility parameters and other cohesion parameters*. Florida: Raton, CRC Press, Inc..

Calvert, P. (1997). Biopolymers: The structure of starch. *Nature*, *389*, 338–339.

Carrado, K. A., Xu, L., Seifert, S., Csencsits, R., & Bloomquist, C. A. A. (2000). Polymer–clay nanocomposites derived from polymer-silicate gels. In T. J. Pinnavaia, & G. Beall (Eds.), *Polymer–clay nanocomposites* (pp. 54–55). Chichester: Wiley.

Chen, B., & Evans, J. R. G. (2005). X-ray diffraction studies and phase volume determinations in poly(ethylene glycol)-montmorillonite nanocomposites. *Polymer International*, *54*(5), 807–813.

Chen, B., & Evans, J.R.G. (in press). Poly(ε-caprolatone)-clay nanocomposites. in press.

De Carvalho, A. J. F., Curvelo, A. A. S., & Agnelli, J. A. M. (2001). A first insight on composites of thermoplastic starch and kaolin. *Carbohydrate Polymers*, *45*, 189–194.

Dixon, W. T., Schaefer, J., Sefcik, M. D., Stejskal, E. O., & McKay, R. A. (1982). Total suppression of sidebands in CPMAS C-13 NMR. *Journal of Magnetic Resonance*, *49*, 341–345.

Gaudel-Siri, A., Brocorens, P., Siri, D., Gardebien, F., Bredas, J.-L., & Lazzaroni, R. (2003). Molecular dynamics study of ε-caprolactone intercalated in Wyoming sodium montmorillonite. *Langmuir*, *19*, 8287–8291.

Gonera, A., & Cornillon, P. (2002). Gelatinization of starch/gum/sugar systems studied by using DSC, NMR, and CSLM. *Starch/Stärke*, *54*, 508–516.

Grim, R. E. (1968). *Clay mineralogy* (2nd ed.). New York: McGraw-Hill Book Company pp. 58, 83, 86.

Jimenez, G., Ogata, N., Kawai, H., & Ogihara, T. (1997). Structure and thermal/mechanical properties of poly(ε-caprolactone)-clay blend. *Journal of Applied Polymer Science*, *35*(2), 2211–2220.

Jinadasa, K. B. P. N., & Dissanayake, C. B. (1992). The effect of selenium on fluoride–clay interactions—possible environmental-health implications. *Environmental Geochemistry and Health*, *14*(1), 3–7.

Krautkrämer, J., & Krautkrämer, H. (1990). *Ultrasonic testing of materials* (4th ed.). Berlin: Springer-Verlag pp. 13, 14, 167.

Krikorian, V., & Pochan, D. J. (2003). Poly(L-lactic acid)/layered silicate nanocomposite: fabrication, characterization and properties. *Chemistry of Materials*, *15*(22), 4317–4324.

Kubies, D., Pantoustier, N., Dubois, P., Rulmont, A., & Jerome, R. (2002). Controlled ring-opening polymerization of ε-caprolactone in the presence of layered silicates and formation of nanocomposites. *Macromolecules*, *35*, 3318–3320.

Ma, X. F., & Yu, J. G. (2004). The plasticizers containing amide groups for thermoplastic starch. *Carbohydrate Polymers*, *57*(2), 197–203.

McGlashan, S. A., & Halley, P. J. (2003). Preparation and characterization of biodegradable starch-based nanocomposite materials. *Polymer International*, *52*, 1767–1773.

Pang, J. T., Fan, C. H., Liu, X. J., Chen, T., & Li, G. X. (2003). A nitric oxide biosensor based on the multi-assembly of hemoglocbin/montmorillonite/polyvinyl alcohol at a pyrolytic graphite electrode. *Biosensors and Bioelectronics*, *19*(5), 441–445.

Park, H.-W., Lee, W.-K., Park, C.-Y., Cho, W.-J., & Ha, C.-S. (2003). Environmentally friendly polymer hybrids Part I mechanical, thermal, and barrier properties of thermoplastic starch/clay nanocomposites. *Journal of Materials Science*, *38*, 909–915.

Park, H.-M., Li, X., Jin, C.-Z., Park, C.-Y., Cho, W. J., & Ha, C.-S. (2002). Preparation and properties of biodegradable thermoplastic starch/clay hybrids. *Macromolecular Materials and Engineering*, *287*, 553–558.

Psomiadou, E., Arvanitoyannis, I., Biliaderis, C. G., Ogawa, H., & Kawasaki, N. (1997). Biodegradable films made from low-density polyethylene, rice starch and potato starch for food packaging applications: Part 2. *Carbohydrate Polymers*, *33*, 227–242.

Qian, D. J., Nakamura, C., Wenk, S. O., Ishikawa, H., Zorin, N., & Miyake, J. (2002). A hydrogen biosensor made of clay, poly(butylviologen), and hydrogenase sandwiched on a glass carbon electrode. *Biosensors and Bioelectronics*, *17*(9), 789–796.

Ray, S. S., Yamada, K., Okamoto, M., Fujimoto, Y., Ogami, A., & Ueda, K. (2002). New polylactide/layered silicate nanocomposites. A novel biodegradable material. *Nano Letters*, *2*(10), 1093–1096.

Ray, S. S., Yamada, K., Okamoto, M., Fujimoto, Y., Ogami, A., & Ueda, K. (2003). New polylactide/layered silicate nanocomposites. 3. High-performance biodegradable materials. *Chemistry of Materials*, *15*, 1456–1465.

Shen, Z., Simon, G. P., & Cheng, Y.-B. (2002). Comparison of solution intercalation and melt intercalation of polymer–clay nanocomposites. *Polymer*, *43*, 4251–4260.

Smits, A. L. M., Ruhnau, F. C., Vliegenthart, J. F. G., & van Soest, J. J. G. (1998). Ageing of starch based systems as observed with FT-IR and solid state NMR spectroscopy. *Starch/Stärke*, *50*(11–12), 478–483.

Tavares, M. I. B., Bathista, A. L. B. S., Silva, E. O., Filho, N. P., & Nogueira, J. S. (2003). A molecular dynamic study of the starch obtained from the Mangifera indica Cv. Bourbon and Espada seeds by C-13 solid state NMR. *Carbohydrate Polymers*, *53*(2), 213–216.

Triantafillidis, C. S., LeBaron, P. C., & Pinnavaia, T. J. (2002). Thermoset epoxy-clay nanocomposites: the dual role of alpha, omega-diamines as clay surface modifiers and polymer curing agents. *Journal of Solid State Chemistry*, *167*, 354–362.

Trommsdorff, U., & Tomka, I. (1995). Structure of amorphous starch. 2. Molecular interactions with water. *Macromolecules*, *28*, 6138–6150.

Wilhelm, H.-M., Sierakowski, M.-R., Souza, G. P., & Wypych, F. (2003). Starch films reinforced with mineral clay. *Carbohydrate Polymers*, *52*, 101–110.